

Dual time-point imaging for post-dose binding potential estimation applied to a [¹¹C]raclopride PET dose occupancy study

Isadora L Alves¹, Antoon TM Willemsen¹, Rudi A Dierckx¹, Ana Maria M da Silva² and Michel Koole^{1,3}

Abstract

Receptor occupancy studies performed with PET often require time-consuming dynamic imaging for baseline and post-dose scans. Shorter protocol approximations based on standard uptake value ratios have been proposed. However, such methods depend on the time-point chosen for the quantification and often lead to overestimation and bias. The aim of this study was to develop a shorter protocol for the quantification of post-dose scans using a dual time-point approximation, which employs kinetic parameters from the baseline scan. Dual time-point was evaluated for a [¹¹C]raclopride PET dose occupancy study with the D2 antagonist JNJ-37822681, obtaining estimates for binding potential and receptor occupancy. Results were compared to standard simplified reference tissue model and standard uptake value ratios-based estimates. Linear regression and Bland–Altman analysis demonstrated excellent correlation and agreement between dual time-point and the standard simplified reference tissue model approach. Moreover, the stability of dual time-point-based estimates is shown to be independent of the time-point chosen for quantification. Therefore, a dual time-point imaging protocol can be applied to post-dose [¹¹C]raclopride PET scans, resulting in a significant reduction in total acquisition time while maintaining accuracy in the quantification of both the binding potential and the receptor occupancy.

Keywords

Dual time-point, positron emission tomography, quantification, binding potential, [¹¹C]raclopride

Received 16 November 2015; Accepted 7 March 2016

Introduction

One of many applications of positron emission tomography (PET) is to investigate the suitability and target engagement of new pharmaceuticals in vivo. With a suitable radiotracer for the same target, PET imaging is able to measure receptor occupancy or enzyme inhibition of a new drug.¹ These studies evaluate the drug's ability to reach its target and determine the proper dosage to reach specific occupancy levels for the intended effect. Therefore, PET dose occupancy studies play an important role in drug advancement by accelerating development in a focused manner and reducing trial costs.²

In order to obtain the relationship between drug concentration in plasma and the achieved percentage of receptor occupancy (Occ%), a multiple-scan PET

occupancy study must be designed. The study design consists of a baseline scan followed by either one or more scans after drug dosing (i.e. post-dose scans). Assuming no change in tracer affinity³ and correcting for possible influence of the drug of interest in the

¹Department of Nuclear Medicine and Molecular Imaging, University of Groningen, University Medical Center Groningen, Groningen, The Netherlands

²Laboratory of Medical Imaging, School of Physics, Pontifícia Universidade Católica do Rio Grande do Sul, Porto Alegre, Brazil

³Department of Nuclear Medicine and Molecular Imaging, KU Leuven, Leuven, Belgium

Corresponding author:

Michel Koole, Department of Nuclear Medicine and Molecular Imaging, KU Leuven, Herestraat 49, B-3000 Leuven, Belgium.

Email: michel.koole@kuleuven.be

delivery of the tracer, the competition between drug and radiolabeled ligand results in a reduction in specific tracer uptake seen in the target in the post-dose scans compared to the baseline. This difference provides information on the amount of receptors occupied by the drug.⁴

When a brain region devoid of the target of interest is available, receptor occupancy can be calculated by using either distribution volume ratio (DVR)⁵ or binding potential (BP_{ND}) estimated from a reference region approach. These models can provide indirect input functions by using information given by the reference region about the tracer's non-specific binding properties. Methods such as the simplified reference tissue model (SRTM)⁶ allow direct estimation of the binding potential from a dynamic scan and therefore contribute to a straightforward quantification of receptor occupancy. However, most reference tissue methods require time-consuming full dynamic scanning protocols.

Reduction in scan duration is of particular interest in drug occupancy studies, as subjects must undergo at least two PET scans per study. Additionally, shorter protocols allow more flexibility in a study set, increase comfort, and lower costs. On that account, approximations have been proposed⁷⁻⁹ in order to obtain the DVR or the BP_{ND} from short static imaging protocols. These relate a late time ratio between tracer uptake in target and reference tissues, expressed in standard uptake values (SUVR), to the receptor imaging parameters. However, such approximations rely on the assumption that the tracer is in transient equilibrium at late time points.⁷ Besides being dependent on the correct determination of the equilibrium period, such methods have been demonstrated to consistently overestimate DVR and BP_{ND}.^{7,8,10}

The aim of this study was to avoid the overestimation associated with SUVR based methods while maintaining short and flexible acquisition protocols. Therefore, an equation relating DVR to SUVR was derived and different methods to calculate the resulting correction term were investigated. The proposed method uses a combination of dynamic baseline and dual time-point static post-dose scans. Although the method still requires dynamic information, it might prove useful in the context of multi-scan protocols, such as dose occupancy studies. Within such a context, it is assumed that the specific kinetic parameters used in the method remain constant between scans. Consequently, the dynamic information necessary for the quantification of the post-dose scans can be extracted from the baseline scans. In this case, BP_{ND} and occupancy values can be estimated from a dynamic baseline and a series of static post-dose scans, thereby reducing the overall acquisition time while maintaining accuracy.

Material and methods

Dual time-point approximation

When the tracer kinetics in the target and reference compartments can be approximated by a one-tissue compartment model (ITCM),³ the SRTM can be applied and the instantaneous change in tracer concentration in each compartment is described by

$$\frac{dC_T(t)}{dt} = K_1^T C_P(t) - k_{2a}^T C_T(t) \quad (1)$$

$$\frac{dC_R(t)}{dt} = K_1^R C_P(t) - k_2^R C_R(t) \quad (2)$$

where $C_P(t)$ is the tracer concentration in plasma, $C_T(t)$ and $C_R(t)$ are the concentrations in target and reference compartments, K_1^T and K_1^R are the rate constants describing the tracer influx from plasma to the respective compartments, k_2^R is the reference washout rate constant from the reference to the plasma, k_{2a}^T is the apparent target washout rate constant, and (t) is time.

The apparent k_{2a}^T of the target compartment describes the overall washout from both the specific and non-displaceable binding parts of the compartment to the plasma and is related to k_2^T as

$$\frac{K_1^T}{k_{2a}^T} = \frac{K_1^T}{k_2^T} \cdot (1 + BP_{ND}) \quad (3)$$

Combining (1) and (2) by isolating $C_P(t)$, dividing both sides of the resulting equation by $C_R(t)$, and assuming the distribution volume of the non-specifically bound tracer is the same in both the target and reference tissues ($K_1^T/k_2^T = K_1^R/k_2^R$) result in

$$\frac{dC_T/dt}{C_R} = \frac{k_2^T}{k_2^R} \left(\frac{dC_R/dt}{C_R} + k_2^R \right) - k_2^T \frac{SUVR}{DVR} \quad (4)$$

where $SUVR = C_T(t)/C_R(t)$ and $DVR = (K_1^T/k_{2a}^T)/(K_1^R/k_2^R) = (K_1^T/k_{2a}^T)/(K_1^T/k_2^T) = k_2^T/k_{2a}^T$. Rearranging the terms, a linear relationship between DVR and SUVR is described by

$$DVR(t) = \frac{SUVR(t)}{1 + \frac{1}{k_2^R} \frac{dC_R(t)/dt}{C_R(t)} - \frac{1}{k_2^T} \frac{dC_T(t)/dt}{C_R(t)}} \quad (5)$$

Equation (5) shows that estimation of DVR requires the determination of (1) the SUVR and (2) a time-dependent correction factor. The second is defined by the slope of target and reference tissue time-activity curves (TAC) normalized to the reference tissue tracer concentration ($dC_R(t)/dt/C_R(t)$ and $dC_T(t)/dt/C_R(t)$), and the washout rate constants of both regions.

For the determination of both the SUVR and the TAC slopes, a dual time-point (DTP) approach is applied.

Taking into account the activity concentration of two scan frames of equal duration, a dual time-point SUVR is calculated as the geometric mean¹¹ of tracer concentration in each frame

$$SUVR(t) = \frac{\sqrt{C_T(t_1) \cdot C_T(t_2)}}{\sqrt{C_R(t_1) \cdot C_R(t_2)}} \quad (6)$$

where t_1 and t_2 are the time-points of the two frames ($t_1 < t_2$) and $t = (t_1 + t_2)/2$.

The normalized slopes, defined by the instantaneous derivatives, are estimated from the same frames by a finite differences approximation

$$\frac{\Delta C_X(t)/\Delta t}{C_R(t)} = \frac{\frac{C_X(t_2) - C_X(t_1)}{t_2 - t_1}}{\sqrt{C_R(t_2) \cdot C_R(t_1)}} \quad (7)$$

where C_X is the tracer concentration in either the target or the reference compartment. The estimation of the washout rate constants (k_2^T and k_2^R) requires information from a dynamic scan and can be determined from the SRTM or approximated by a population-based average, as is the case for the Logan reference tissue model.⁵ In the setting of a PET dose occupancy study, a full dynamic baseline scan together with the correspondent washout rate constants is available. Assuming the individual kinetic parameters to be stable over time, the SRTM model can be applied to the baseline scan in order to determine the washout rate constants used in equation (5). This provides a subject-specific approximation for the quantification of post-dose scans.

Using equations (6) and (7) and the baseline-derived washout rate constants for the determination of DVR, equation (5) can be determined from a dual time-point approximation, yielding DVR_{DTP} or the corresponding binding potential BP_{DTP} ($BP_{DTP} = DVR_{DTP} - 1$).

Therefore, with the proposed method, receptor occupancy values for post-dose scans are calculated based on the following definition

$$\%Occ_{DTP} = \left(1 - \frac{BP_{DTP}(post - dose)}{BP_{ND}(baseline)}\right) \cdot 100\% \quad (8)$$

Study setup

The dual time-point method was evaluated by analyzing retrospective data from an open-label PET study that assessed the D2-receptor occupancy after single and multiple doses of 10 mg JNJ-37822681, as

described previously.^{29,30} The study was conducted in the University Medical Center Groningen (UMCG) PET center and was supported by Xendo Drug Development (Groningen, The Netherlands). Ethics committee approval was obtained (Stichting Beoordeling Ethiek Biomedisch Onderzoek, Assen, the Netherlands) and all subjects gave prior written informed consent after receiving detailed information about the protocol, in accordance with the ethical standards of the Helsinki Declaration of 1964 and its later amendments. The study population consisted of 11 healthy male subjects with ages ranging from 18 to 55 years, and a body mass index from 18 to 30 kg/m².

All subjects underwent a structural T1-weighted MRI scan to enable image coregistration for the analysis. A baseline and two post-dose scans were performed, except for two occasions of tracer synthesis failure, totaling 31 scans (11 baseline and 20 post-dose). The baseline [¹¹C]raclopride PET scans were acquired between 25 and 2 days prior to JNJ-37822681 dosing (day 1). Next, subjects received 10 mg of the compound twice a day, on days 1–6, and a single dose in the morning of day 7. On day 1, the first post-dose [¹¹C]raclopride PET scans were performed 2.1 to 10.6 h after administration of the compound. During days 7–10, the second post-dose [¹¹C]raclopride PET scans were obtained 2.6–58.5 h after dosing on day 7.

Dynamic [¹¹C]raclopride PET imaging and analysis

All PET scans were performed with a high-resolution ECAT EXACT HR+ scanner (Siemens Healthcare, Erlangen, Germany). Individual 2D ⁶⁸Ge-based transmission scans of 10 min were acquired for attenuation correction. Both at baseline and post-dose scans subjects received an intravenous bolus injection of 200 MBq of [¹¹C]raclopride and underwent a 60 min dynamic PET acquisition, starting at the time of injection and consisting of 21 frames (6 × 5 s, 3 × 10 s, 4 × 60 s, 2 × 150 s, 2 × 300 s, and 4 × 600 s). Each emission frame was corrected for decay, scatter, randoms, and attenuation, and reconstructed using the ordered subset expectation maximization (OSEM) algorithm (four iterations and 16 subsets) followed by a 4 mm FWHM Gaussian smoothing.

For each subject, summed PET images were coregistered to corresponding MRI, and MRI data were subsequently normalized to MNI space using the T1 MRI template available in PMOD (version 3.3, PMOD Technologies Ltd, Zurich, Switzerland). The same coregistration and normalization parameters were then applied to the dynamic scans. Time-activity curves were generated for striatum and cerebellum¹⁴ by applying the corresponding predefined volumes of interest (VOIs) of the Hammers atlas¹⁵ to the dynamic data.

Following the well validated quantification approach for [^{11}C]raclopride,⁶ the simplified reference tissue model was defined as the standard method. The extracted TACs from baseline and post-dose scans were fitted to the SRTM using cerebellum as a reference region, and BP_{ND} values were generated for the striatum. Washout rate constants for both striatum (k_2^T) and cerebellum (k_2^R) were also recorded for all scans. Corresponding receptor occupancy estimates based on baseline and post-dose BP_{ND} were computed.

Dual time-point image analysis

From the same time–activity curves, the dual time-point approximation was implemented in two steps. First, the scan-specific SRTM-derived washout rate constants k_2^T and k_2^R were used in equation (5) in order to mathematically validate the method and evaluate the effect of using a finite difference approximation for the estimation of TAC slopes. Binding potential computed from this first step is hereby defined as finite differences binding potential (BP_{FD}). Additionally, an error analysis¹⁶ was performed to assess the effect of changes (up to $\pm 30\%$) in the kinetic parameters which could be related to perfusion differences between baseline and post-dose scans. The changes in k_2^T and k_2^R can be related to a global difference in perfusion between scans, while changes in R_1 can be induced by a relative change in perfusion between target and reference tissue. These changes in kinetic parameters were tested in increments of 10% and corresponding errors in binding potential estimates recorded. Next to this error analysis, the effect of noise on DTP based BP_{FD} estimates was assessed and compared to the impact of noise on SRTM BP_{ND} and SUVR estimates. For this purpose, a noise-free TAC for the reference tissue was defined as the average curve of all cerebellar TACs and two noise-free target TACs were generated using SRTM and the average striatal SRTM kinetic parameters of the baseline ($R_1 = 0.89$, $k_2^T = 0.20$, $\text{BP}_{\text{ND}} = 2.35$) and post-dose scans ($R_1 = 0.89$, $k_2^T = 0.21$, $\text{BP}_{\text{ND}} = 1.44$). Next, Poisson-like noise accounting for frame duration and decay¹⁷ was added to the noise-free data by generating random numbers from a normal distribution with zero mean and a standard deviation corresponding to 5%, 10%, and 15% of the average uptake value of the last two frames. For each of the three noise levels, 1000 TACs were generated and used for binding potential and SUVR estimation.

Next, the dynamic baseline-derived washout rate constants were applied to the post-dose scans and DVR_{DTP} values were determined. Binding potential obtained from this method is hereby defined as dual time-point binding potential (BP_{DTP}). Corresponding receptor occupancy estimates ($\%\text{Occ}_{\text{DTP}}$) were computed based on SRTM BP_{ND} from the baseline scan

and BP_{DTP} from the post-dose scan using equation (8) and compared to $\%\text{OccBPND}$ using SRTM BPND values of both baseline and post-dose scans. Finally, a population-based approach for the estimation of BP_{DTP} , denoted BP_{POP} , was evaluated as a potential method for completely avoiding dynamic scans. In this step, individual k_2^T and k_2^R values were replaced by population based averages for the determination of both baseline and post-dose BP_{DTP} estimates.

For comparison, a simple tissue concentration ratio (SUVR) was calculated for all scans and evaluated as a method for binding potential estimation by assuming a direct correspondence between SUVR and DVR. Binding potential estimated from this approximation is hereby defined as SUVR binding potential (BP_{SUVR}). Corresponding receptor occupancy ($\%\text{Occ}_{\text{SUVR}}$) was calculated from baseline and post-dose BP_{SUVR} and compared to $\%\text{OccBPND}$ using SRTM BPND values of both baseline and post-dose scans.

Three different combinations of two consecutive 10-min time frames (20–40 min, 30–50 min, and 40–60 min) were chosen for all approximations in order to evaluate the time dependency in the accuracy of each method.

Statistical analysis

Results are reported as mean \pm standard deviation (SD). Correlation between SRTM BP_{ND} and all other approximations was assessed by linear regression analysis. The agreement between methods and the bias associated with the approximations were determined based on a Bland–Altman analysis on binding potential and receptor occupancy estimates. Limits of agreement of 95% were considered. The results of quantification of simulated noisy data by each of the three methods (SRTM, DTP or SUVR) were compared to noise-free SRTM BP_{ND} values via two measures: $\%\text{bias}$, calculated as $(\bar{X}_{\text{noise}} - X)/X * 100$ and $\%\text{SD}$, calculated as $SD(X_{\text{noise}})/X * 100$, where X_{noise} represents the DTP BP_{FD} , SRTM BP_{ND} , and SUVR estimates obtained using the simulated noise TACs while X represents the underlying noise-free value.

Changes in bias associated with different time intervals were analyzed to determine whether the methods are time-dependent. Further analysis was also performed on k_2^T and k_2^R values to determine whether there was a significant difference in the individual kinetic parameters between baseline and post-dose scans. Due to the presence of repeated measurements and incomplete data (two failed post-dose scans), the Generalized Estimating Equations (GEE) model¹⁸ was applied to both analysis, and the Wald test was used to report resulting p-values.

All statistical analysis was performed using IBM SPSS Statistics (Version 20.0, Armonk, NY) and GraphPad Prism (Version 5.0, San Diego, CA, USA), and a $p < 0.05$ was considered significant in all tests.

Results

Binding potential estimation

BP_{FD} showed a perfect correlation ($R^2 = 1$) with SRTM derived BP_{ND} for all time intervals (Figure 1(a)). Bland–Altman analysis showed a negligible bias and

95% limits of agreement of less than $\pm 1\%$ for all time intervals (Table 1), supporting the use of the finite differences approximation for the determination of the TAC slopes as presented in Figure 2. Moreover, a perfusion-related error analysis showed that potential changes in kinetic parameters between scans would result in less than 8% error in BP_{DTP} estimation (Figure 3(a) and (b)). The highest percentage of error in the estimation of binding potential (7.4%) resulted from a 30% decrease in k_2^T and k_2^R values, while the corresponding levels of change in R_1 values had an effect of only 4% in BP_{DTP} values.

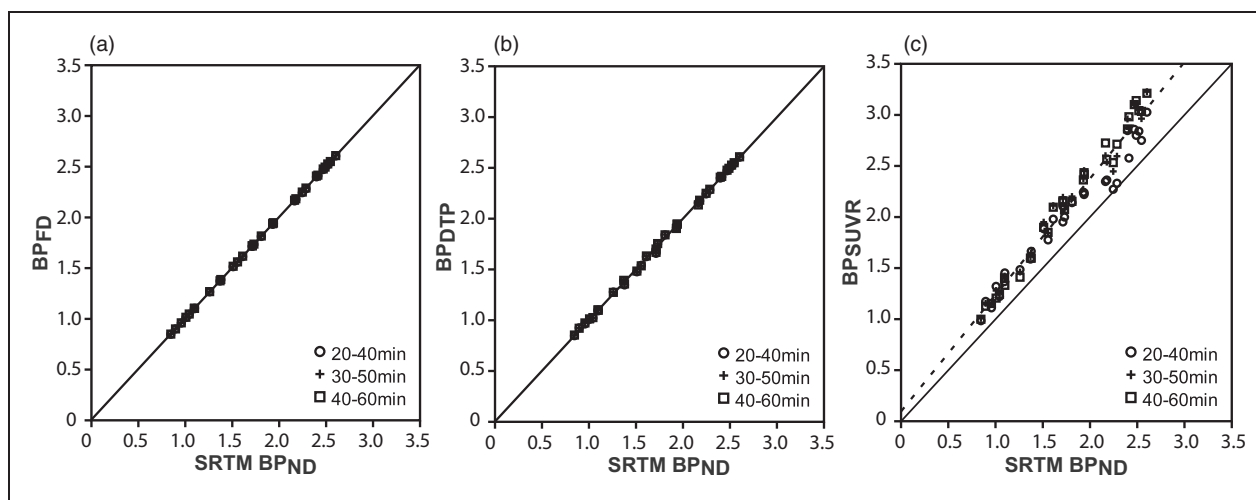


Figure 1. Regression analysis of binding potential estimates. Regression analysis of BP_{FD} , BP_{DTP} and BP_{SUVR} with SRTM BP_{ND} . Identity line is shown as reference. BP_{FD} shows perfect correlation with SRTM BP_{ND} , with a $R^2 = 1$ and slope = 1 for all time frames (a). BP_{DTP} shows excellent correlation with SRTM BP_{ND} , demonstrated by a $R^2 = 0.99$ and slope = 0.99 for all time frames (b). BP_{SUVR} shows good correlation and a small overestimation when compared to SRTM BP_{ND} , presenting a $R^2 = 0.97$ and slope = 1.02 for the 20–40 min, $R^2 = 0.98$ and slope = 1.18 for the 30–50 min and $R^2 = 0.99$ and slope = 1.23 for the 40–60 min frames (c).

Table 1. Bland–Altman analysis of binding potential estimates.

| Approximation compared to SRTM BP_{ND} | Frames (min) | | |
|--|-----------------|------------------|-------------------|
| | 20–40 | 30–50 | 40–60 |
| BP_{FD} | | | |
| Bias (%) | 0.17 ± 0.22 | 0.38 ± 0.22 | 0.44 ± 0.18 |
| 95% limits of agreement (%) | $-0.25-0.61$ | $-0.05-0.82$ | $0.09-0.81$ |
| BP_{DTP} | | | |
| Bias (%) | 0.27 ± 0.22 | 0.48 ± 0.21 | 0.52 ± 0.17 |
| 95% limits of agreement (%) | $-0.16-0.71$ | $0.06-0.91$ | $0.19-0.86$ |
| BP_{SUVR} | | | |
| Bias (%) | 15.1 ± 6.45 | 19.9 ± 4.21 | 19.4 ± 3.57 |
| 95% limits of agreement (%) | $2.45-27.7$ | $11.60-28.14$ | $12.41-26.41$ |
| BP_{POP} | | | |
| Bias (%) | 0.01 ± 1.36 | -0.13 ± 1.26 | -0.19 ± 1.10 |
| 95% limits of agreement (%) | $-2.67-2.68$ | $-2.62-2.35$ | -2.36 to 1.97 |

Note: Bland–Altman analysis comparing standard SRTM based BP_{ND} values to estimates from other approximations. Bias and 95% limits of agreement expressed in percentage difference plus or minus the standard deviation.

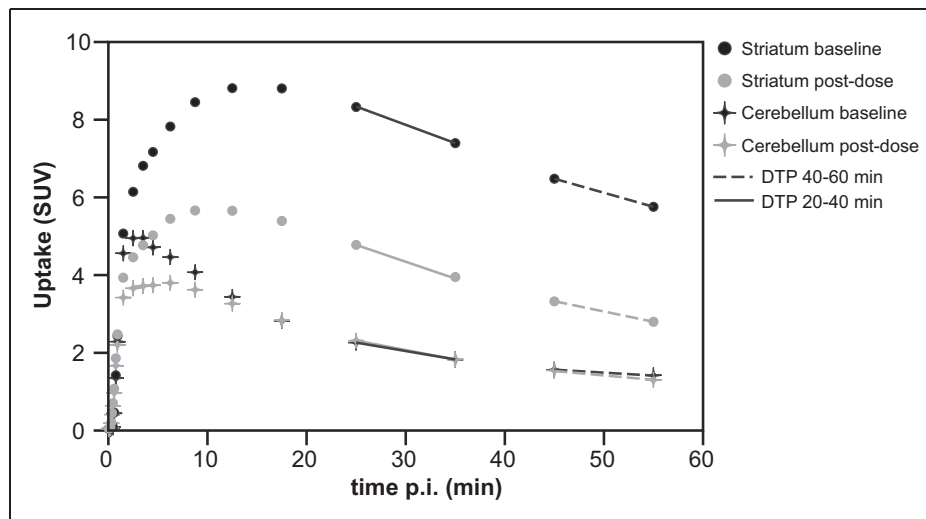


Figure 2. Representation of the method's approximation. Representative TAC for both baseline and post-dose scans of a subject with the highest occupancy levels, demonstrating the estimation of the TAC slopes by the finite differences approximation.

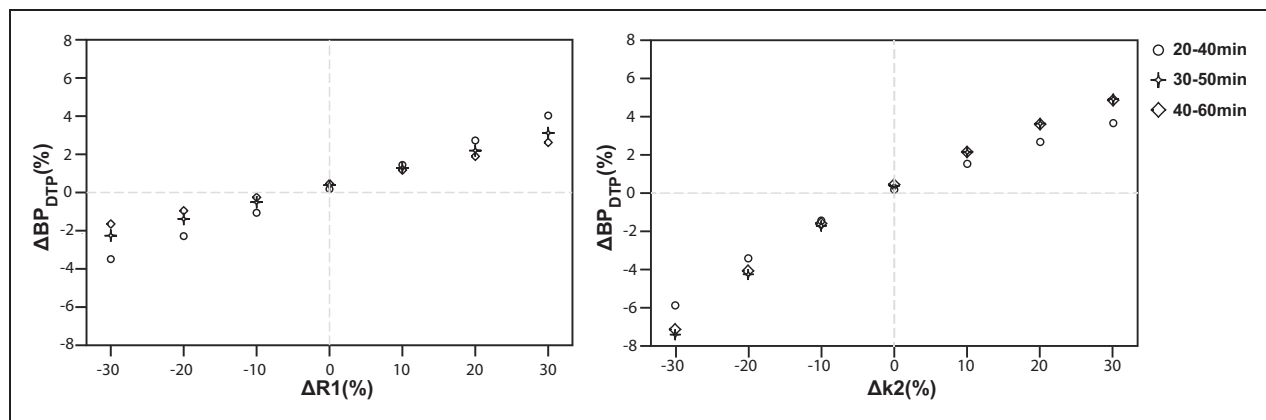


Figure 3. Kinetic parameter estimation error analysis. Error analysis performed on changes in R_1 and k_2^T and k_2^R of up to $\pm 30\%$ between baseline and post-dose scans. The percentage error in BP_{DTP} estimation is less than 5% for changes in R_1 (a) and less than 8% for changes in k_2^T and k_2^R (b).

The results of the estimation of BP_{FD} from simulated noisy data showed that for the DTP method, the %bias ranged from 0.25 to 1.3% for the lowest level (5%), increasing from 3.8 to 10.1% for the highest noise level (15%), while the %SD ranged from 7.4 to 13% for the lowest level (5%) of simulated TACs to 24 to 50% for the 15% noise level. On the other hand, SRTM BP_{ND} and SUVR estimates using the simulated, noisy TACs resulted in a %bias of less than 4% and a maximum %SD of less than 16% for all noise levels. Representative TACs for the 15% noise simulation are shown in Figure 4 and an overview of noise-induced bias and variability for the different methods is presented in Table 2.

Using subject-specific k_2^T and k_2^R values, determined at baseline, resulted in excellent correlation ($R^2=0.99$)

between post-dose BP_{DTP} and SRTM BP_{ND} (Figure 1(b)). The linear regression demonstrates excellent agreement between the two methods. The bias corresponding with the new method remained negligible and Bland–Altman analysis showed the same 95% limits of agreement of less than $\pm 1\%$ for all time intervals (Table 1).

The results from the GEE analysis on the change of kinetic parameters from baseline to post-dose scans were in accordance with our assumption, demonstrating that individual k_2^T and k_2^R values are not significantly different between scans ($p=0.81$). Moreover, the inter-subject variation in washout rate constant values is small across scans, with baseline values of $k_2^T=0.20 \pm 0.02 \text{ min}^{-1}$ and $k_2^R=0.23 \pm 0.01 \text{ min}^{-1}$, and post-dose values of $k_2^T=0.21 \pm 0.01 \text{ min}^{-1}$ and

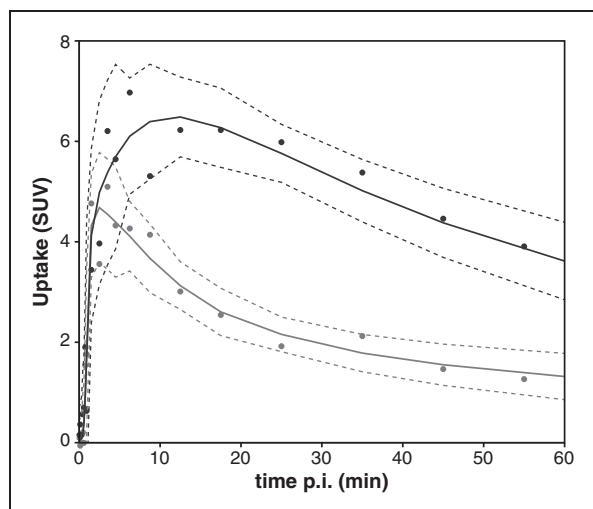


Figure 4. Representative noise simulations for striatal and cerebellar TACs. A representation of the noise free post-dose striatal (black) and cerebellar (gray) TACs used for the noise simulation (solid lines) together with representative TACs for the 15% noise level (dots) and their upper and lower bounds, defined as $\pm 1.96 \times \text{SD}$ (dashed lines).

$k_2^R = 0.23 \pm 0.03 \text{ min}^{-1}$ for the first post-dose and $k_2^T = 0.21 \pm 0.02 \text{ min}^{-1}$ and $k_2^R = 0.23 \pm 0.03 \text{ min}^{-1}$ for the second post-dose scan. In terms of relative changes between baseline and post-dose scans, k_2^R values changed $1.67 \pm 8.45\%$ (range: -12.80% to 17.64%) while R_1 values changed $0.42 \pm 5.81\%$ (range: -7.50% to 11.16%). Next to these results, the population-based average approach BP_{POP} demonstrated high correlations with SRTM BP_{ND} for all time intervals ($R^2 = 0.99$) and a corresponding bias of less than 0.2% (Table 1).

Binding potential values obtained from the SUVR method also demonstrated high correlation ($R^2 = 0.97$ – 0.99) with SRTM-derived estimates although with a consistent overestimation for all time intervals (Figure 1(c)). In fact, the average factor for correction of SUVR (denominator in equation (5)) was 1.14 for the first post-dose scan (40–60 min interval as an example). It was composed of an average slope of $-0.058 \pm 0.014 \text{ g ml}^{-1} \text{ min}^{-1}$ and $-0.014 \pm 0.004 \text{ g ml}^{-1} \text{ min}^{-1}$ for striatum and cerebellum respectively, a $C_R = 1.51 \pm 0.21 \text{ g ml}^{-1}$ and the $k_2^T = 0.21 \pm 0.01 \text{ min}^{-1}$ and

Table 2. Noise-induced bias and variability.

| %noise | Model | Frames (min) | Baseline | | Post dose | | |
|-----------------------------|------------------------------|------------------------------|----------|-------|-----------|-------|-------|
| | | | %bias | %SD | %bias | %SD | |
| 5% | SRTM BP_{ND} | 0–60 | 0.02 | 3.36 | –0.38 | 3.95 | |
| | | 20–40 | 0.09 | 2.50 | 0.08 | 2.55 | |
| | | 30–50 | 0.13 | 3.20 | 0.09 | 3.42 | |
| | | 40–60 | 0.21 | 4.04 | 0.09 | 4.25 | |
| | DTP BP_{FD} | 20–40 | 0.48 | 7.37 | 0.25 | 7.72 | |
| | | 30–50 | 0.32 | 8.77 | 0.60 | 10.27 | |
| 10% | SRTM BP_{ND} | 0–60 | 0.04 | 6.73 | –1.79 | 10.99 | |
| | | 20–40 | 0.47 | 5.17 | 0.30 | 5.18 | |
| | | 30–50 | 0.64 | 6.42 | 0.46 | 6.74 | |
| | | 40–60 | 0.65 | 8.36 | 0.76 | 8.58 | |
| | DTP BP_{FD} | 20–40 | 2.26 | 15.35 | 1.66 | 16.09 | |
| | | 30–50 | 1.74 | 18.57 | 1.72 | 19.89 | |
| | | 40–60 | 3.63 | 25.39 | 4.81 | 28.56 | |
| | 15% | SRTM BP_{ND} | 0–60 | –1.14 | 12.54 | –3.03 | 15.83 |
| | | | 20–40 | 0.63 | 7.58 | 0.92 | 8.10 |
| 30–50 | | | 0.74 | 9.94 | 1.29 | 10.16 | |
| 40–60 | | | 1.54 | 12.87 | 1.50 | 13.53 | |
| DTP BP_{FD} | | 20–40 | 3.82 | 24.00 | 4.51 | 25.44 | |
| | | 30–50 | 4.78 | 33.18 | 4.60 | 32.72 | |
| | | 40–60 | 10.11 | 43.20 | 9.63 | 50.70 | |

Note: Comparison of the noise-induced bias and variability between different quantification methods applied to simulated noisy TACs. The analysis was performed for three different noise levels (5%, 10%, and 15%) of noise-free TACs representative for baseline ($\text{BP}_{\text{ND}} = 2.35$) and post dose ($\text{BP}_{\text{ND}} = 1.44$) scanning.

$k_2^R = 0.23 \pm 0.03 \text{ min}^{-1}$. Bland–Altman analysis showed a more pronounced bias associated with this method (Table 1). In addition, the GEE analysis showed that the time interval is a significant factor ($p < 0.05$) for bias. No significant difference was found between the 30–50 min and 40–60 min estimates, while the bias associated with the 20–40 min interval was significantly different from the other two intervals ($p = 0.01$ in relation to 30–50 min and $p = 0.02$ in relation to 40–60 min).

Receptor occupancy estimation

The range of receptor occupancy achieved in this study, calculated from SRTM derived BP_{ND} , was from 0% at baseline up to 65.7% in post-dose scans, with an average value of $\% \text{Occ} = 38.3 \pm 18.5\%$.

Receptor occupancy determined from post-dose BP_{DTP} showed small bias and excellent agreement to the standard method. Furthermore, the values for $\% \text{Occ}_{\text{DTP}}$ were not affected by the choice of time post-injection, being consistent for all three dual time-point combinations chosen in this work (bias of $0.16 \pm 0.97\%$ for 20–40 min, $0.08 \pm 1.01\%$ for 30–50 min and $0.04 \pm 0.92\%$ for 40–60 min, and respective 95% limits of agreement of -1.75% to 2.08% , -1.90% to 2.07% and -1.77% to 1.85%). A representative Bland–Altman plot is shown in Figure 5(a) (40–60 min interval).

Even though BP_{SUVR} in general overestimated SRTM values, the subsequent estimation of receptor occupancy is less affected. Bland–Altman analysis showed a bias of $-4.95 \pm 3.87\%$ for 20–40 min, $-1.76 \pm 3.10\%$ for 30–50 min and $-0.33 \pm 2.44\%$ for 40–60 min, while the corresponding 95% limits of agreement were from -12.2% to 2.98% , -7.85% to 4.31% , and -5.15% to 4.46% . A representative Bland–Altman plot is shown in Figure 5(b) (40–60 min interval).

Discussion

This study aimed at increasing schedule flexibility for post-dose scans in terms of imaging availability, patient comfort, and possible issues with motion artefacts. The proposed method reduces acquisition time for post-dose scanning and eliminates the need to start the post-dose scan at the time of tracer bolus injection. As such, the method allows for the scan to be reset in case of camera failure or patient discomfort, maintaining the validity of the acquired data. Short post-dose scans would also allow PET dose occupancy scans to be performed within a clinical time slot for whole body PET/CT scanning such that these studies can easily blend in with the clinical routine. Besides, the reduction in acquisition time would be beneficial for both imaging staff and volunteers, since motion during scanning

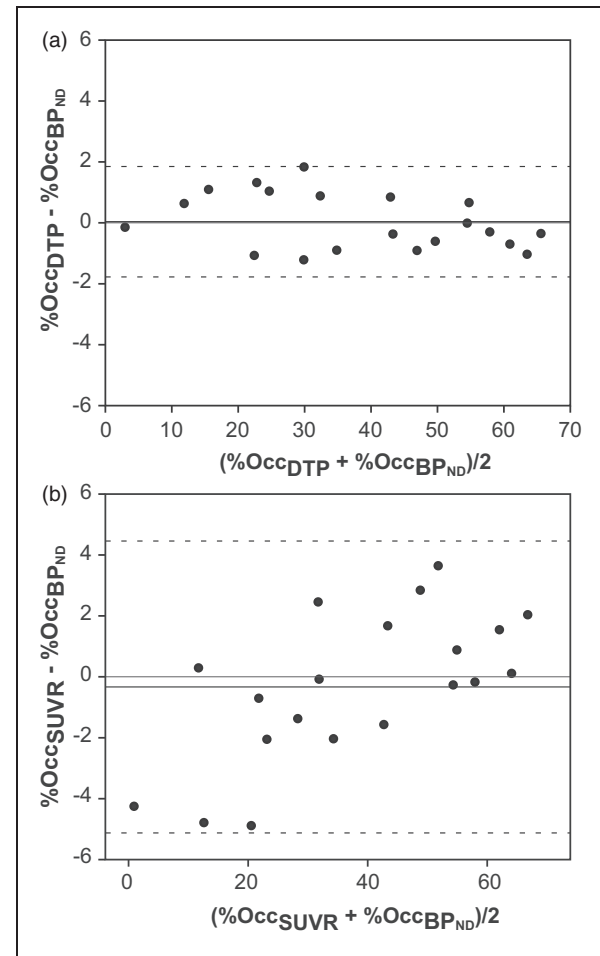


Figure 5. Bland–Altman plots of receptor occupancy estimates. Representative Bland–Altman plots showing agreement between methods for estimation of receptor occupancy and the standard SRTM BP_{ND} based approach. The 40–60 min dual time-point interval was chosen as representative for receptor occupancy estimation using baseline SRTM BP_{ND} and post-dose BP_{DTP} (a) and baseline and postdose BP_{SUVR} (b).

would be reduced and the quantitative quality of the PET data increased, while adding extra flexibility to patient preparation and positioning in the PET system. Moreover, the possible time reduction could also effectively increase the number of subjects scanned per tracer production batch. Indeed, when a standard 60 min dynamic scanning protocol is reduced to a 20 min DTP protocol and, for example, a fixed DTP interval of 20–40 min after injection is chosen for each scan, two consecutive scans can be performed with only a small delay between injections, resulting in the possibility of scanning at least two patients from one $[^{11}\text{C}]$ raclopride tracer batch with a realistic amount of (specific) activity.

The new method is based on a dynamic baseline and a dual time-point approximation for quantification of the post-dose scan. Starting from the same kinetic assumptions as for the SRTM, the method depends on two additional assumptions. The first is that the derivatives of the target and reference TAC slopes can be approximated by a finite difference. The second is that the specific kinetic parameters (k_2^T and k_2^R) of the dynamic baseline scan can be used for the static post-dose scans. These assumptions were evaluated for a PET dose occupancy study with [^{11}C]raclopride, for which the SRTM is considered as a standard and validated approach for BP_{ND} quantification.^{19,20}

The validity of the first assumption was assessed using data from baseline and post-dose scans. Scan-specific washout rate constants k_2^T and k_2^R were obtained from the SRTM fit to the dynamic data, and combined with the finite difference approximation of the TAC slopes for the estimation of BP_{FD} . Bland–Altman comparison of both values for all 31 scans revealed negligible bias and variability, proving excellent agreement between the standard and finite differences based approximation. Taking into account the wide range of occupancy levels for this study, and therefore the wide range of tracer uptake levels in the target region, these results demonstrate the marginal impact of different noise levels on the derivative terms. In this work, data from two consecutive frames of 10 min each were acquired with a Siemens ECAT EXACT HR+ scanner and, noting that current state of the art PET systems provide overall better sensitivity,²¹ even shorter protocols or a reduction in administered dose could be considered. Moreover, we have previously validated the approach for [^{11}C]PIB brain PET imaging where SUVR could be accurately corrected to DVR values with comparable correction factors.²² In terms of the impact of noise, our simulations show that the DTP approach is more sensitive to noise when compared to SRTM BP_{ND} and SUVR estimates, both in terms of bias and variability. For the DTP approach, a 5% noise level is still acceptable in terms of variability (see results in Table 2) while higher noise levels have a considerable impact on the rescaling factor of equation (5). In general, TACs related to lower uptake values of the post-dose scans are less impacted in terms of bias and variability compared to baseline data, while these measures gradually increase for both DTP BP_{FD} and SUVR estimates when later time frames are used. Therefore, DTP is better suited for high uptake tracers and regions with satisfactory count statistics. On the other hand, PET cameras are continuously gaining in sensitivity, resulting in less noisy datasets, while acquisition and reconstruction protocols can be optimized for a DTP approach by improving spatio-temporal filtering after

reconstruction²³ or by increasing the interval between the time frames and therefore extending their duration for the DTP approach. As shown, SUVR is less sensitive to noise since it is based on the geometric mean, but may show an intrinsic bias. SRTM is also less sensitive to noise since it uses all data but, therefore, is not an alternative to DTP.

After validation of the first assumption, the applicability of the proposed method was assessed by evaluating the second assumption. Applying subject-specific k_2^T and k_2^R values determined at baseline to obtain post-dose BP_{DTP} quantification and comparing these with post-dose SRTM BP_{ND} values again revealed negligible bias and variability (Figure 1(b)). These results are in line with the error analysis that was performed on possible changes in k_2^T and k_2^R and in R_1 values between baseline and post-dose scans since the observed range of relative changes for both k_2^R and R_1 would imply a relative BP_{DTP} error of only a few percent. Bland–Altman confidence intervals also did not change when using baseline washout constants in the quantification of post-dose scans, implying their valid use as an approximation for post-dose parameters. These findings are supported by the results of the GEE analysis of the change of k_2^T and k_2^R from baseline to post-dose scans. The within-subject time dependence was found to be not significant, demonstrating the applicability of the proposed method for this study setup. Moreover, the already excellent agreement seen between post-dose BP_{DTP} and SRTM BP_{ND} translates well in terms of receptor occupancy. When comparing receptor occupancy obtained from the standard SRTM method and those where BP_{DTP} was used as an approximation for the post-dose BP_{ND} , the 95% limits of agreement of the difference in receptor occupancy are less than $\pm 2\%$ (Figure 5(a)). This is well within the acceptable range considering the [^{11}C]raclopride studies show a test–retest of up to 8% in striatal binding potential estimates.²⁴

In contrast, BP_{SUVR} estimates suffer from a consistent overestimation which can be seen by both the linear regression analysis (Figure 1(c)) and the bias in binding potential estimation from the SUVR method (Table 1), in agreement with previous studies.^{8,10} However, receptor occupancy estimates are less affected (Figure 5(b)). Nevertheless, the GEE analysis demonstrated that time is a significant factor in bias for this method. Even when measuring SUVR during the transient equilibrium, the overestimation is dependent on the rate of plasma clearance and the tissue kinetics.⁷ In the case of [^{11}C]raclopride, the tissue clearance is fast compared to the plasma clearance, resulting in a small overestimation of V_T from ratio methods.

The dual time-point method increases accuracy, reduces bias, and eliminates the time dependence of

parameter estimation when compared to SUVR methods. It also accounts for errors in the determination of the transient equilibrium state for the scan acquisition, by including the difference in TAC slopes in the determination of DVT_{DTP} (equation (5)). Consequently, DTP protocols offer the possibility of starting the scan at different time points post-injection, avoiding issues related to camera failure. The comparison between post-dose BP_{DTP} and SRTM BP_{ND} and the respective receptor occupancy estimates support the applicability of a shorter protocol in [^{11}C]raclopride dose occupancy studies. Furthermore, an inter-subject variability of $\pm 10\%$ in washout rate constants together with correction factors in the order of 10–18% seen in this work suggest that k_2^T and k_2^R are not the main factors for the correction of these scans and therefore could be approximated by a population average. This was confirmed by our results, suggesting that the baseline scan could also be reduced to a short static scan and the DTP method could be considered as a general alternative approach for the estimation of binding potential values from a bias-corrected SUVR, therefore fully surpassing the need for dynamic scans. For this approach, however, it is necessary to assure that inter-subject variability of these washout rate constants within the study population is limited. While [^{11}C]raclopride is a stable and reliable tracer in terms of quantification,^{24–26} this might not be the case for a larger and heterogeneous study population or for other tracers. In this context, the proposed error analysis can be valuable for determining the impact of the variability of washout rate constants between and within subjects over time²⁷ on the DTP estimates of the binding potential.

Specifically for dose occupancy studies, results depend on the stability of receptor affinity,³ while dosing with new drug compounds may also influence the kinetic behavior of the tracer, compromising the use of baseline washout rate constants for post-dose quantification. Especially regarding the possible effects of the drug dosing on perfusion-related kinetic parameters, a first validation of the approach is necessary. Again, an error analysis similar to the one performed in this study can be valuable to assess the robustness and applicability of this approach in other settings. Moreover, this analysis is rather straightforward provided dynamic baseline datasets are available. On the other hand, simultaneous PET/MRI could be of interest for monitoring of perfusion changes between scans by combining PET with MR ASL (Arterial Spin Labeling) perfusion measurements,²⁸ a perfusion-weighted MR imaging technique that does not require an exogenous contrast agent. Next to dose occupancy studies, the DTP approximation of BP_{ND} could also be a valuable approach for PET displacement or

activation studies where the endogenous neurotransmitter level is increased during scanning and kinetics of specifically bound radioligands are altered. In general, these data are analyzed by an extension of SRTM which models the change of the endogenous neurotransmitter level and quantifies the amplitude of this change. For these studies, a DTP approximation could be considered to monitor BP_{ND} changes relative to baseline after activation.²⁹

To conclude, combining dynamic baseline scanning and dual time-point post-dose imaging resulted in an accurate method for the quantification of BP_{ND} and occupancy levels of the specific and fast-dissociating D2 antagonist JNJ-37822681, using [^{11}C]raclopride PET. Compared to SUVR, the proposed method is more accurate, less time-dependent and produces smaller bias, while the reduction of the total acquisition time is still significant. Although the dual time-point approximation should be applicable to every tracer with a reference tissue and single compartment tracer kinetics, this approach should be validated for dose occupancy studies with other tracers or drug compounds to assess time stability of washout rate constants, and the possible impact of the tested drug on tracer kinetics.

Funding

The author(s) received no financial support for the research, authorship, and/or publication of this article.

Acknowledgements

The authors would like to acknowledge Janssen R&D (Janssen Research and Development, Janssen Pharmaceutica NV, Belgium) for the collaboration which enabled this study. For their support and contribution to the design of the study, a personal acknowledgement is also due to Erik Mannaert, Mark Schmidt and Peter de Boer.

Declaration of conflicting interests

The author(s) declared no potential conflicts of interest with respect to the research, authorship, and/or publication of this article.

Authors' contributions

ILA and MK jointly developed the concept and design of the manuscript. AW and AMMdS contributed greatly to a discussion of the method and its applications. ILA wrote the first draft and searched for relevant articles. RD, MK, AW, and AMMdS reviewed the choice of references, tables, and figures and edited the initial draft and every subsequent draft.

References

1. Matthews PM, Rabiner I and Gunn R. Non-invasive imaging in experimental medicine for drug development. *Curr Opin Pharmacol* 2011; 11: 501–507.

2. Waarde AV. Measuring receptor occupancy with PET. *Curr Pharm Des* 2000; 6: 1593–1610.
3. Innis RB, Cunningham VJ, Delforge J, et al. Consensus nomenclature for in vivo imaging of reversibly binding radioligands. *J Cereb Blood Flow & Metab* 2007; 27: 1533–1539.
4. Willemsen ATMW and Paans AMJ. An introduction to kinetic modeling and quantification and its role in drug development. In: *Trends on the role of PET in drug development*. Singapore: World Scientific Publishing, 2012, pp.417–454.
5. Logan J, Fowler JS, Volkow ND, et al. Distribution volume ratios without blood sampling from graphical analysis of PET data. *J Cereb Blood Flow Metab* 1996; 16: 834–840.
6. Lammertsma AA and Hume SP. Simplified reference tissue model for PET receptor studies. *Neuroimage* 1996; 4: 153–158.
7. Carson RE, Channing MA, Blasberg RG, et al. Comparison of bolus and infusion methods for receptor quantitation: application to [18F]cyclofoxy and positron emission tomography. *J Cereb Blood Flow Metab* 1993; 13: 24–42.
8. Lammertsma AA, Bench CJ, Hume SP, et al. Comparison of methods for analysis of clinical [11C]raclopride studies. *J Cereb Blood Flow Metab* 1996; 16: 42–52.
9. Passchier J, Gee A, Willemsen A, et al. Measuring drug-related receptor occupancy with positron emission tomography. *Methods* 2002; 27: 278–286.
10. Ito H, Hietala J, Blomqvist G, et al. Comparison of the transient equilibrium and continuous infusion method for quantitative PET analysis of [11C]raclopride binding. *J Cereb Blood Flow Metab* 1998; 18: 941–950.
11. Fleming PJ and Wallace JJ. How not to lie with statistics: the correct way to summarize benchmark results. *Commun ACM* 1986; 29: 218–221.
12. Schmidt ME, De Boer P, Andrews R, et al. D2-receptor occupancy measurement of JNJ-37822681, a novel fast off-rate D2-receptor antagonist, in healthy subjects using positron emission tomography: Single dose versus steady state and dose selection. *Psychopharmacology (Berl)* 2012; 224: 549–557.
13. te Beek ET, de Boer P, Moerland M, et al. In vivo quantification of striatal dopamine D2 receptor occupancy by JNJ-37822681 using [11C]raclopride and positron emission tomography. *J Psychopharmacol* 2012; 26: 1128–1135.
14. Hall H, Köhler C, Gawell L, et al. Raclopride, a new selective ligand for the dopamine-D 2 receptors. *Prog Neuropsychopharmacol Biol Psychiatry* 1988; 12: 559–568.
15. Hammers A, Allom R, Koeppe MJ, et al. Three-dimensional maximum probability atlas of the human brain, with particular reference to the temporal lobe. *Hum Brain Mapp* 2003; 19: 224–247.
16. van Berckel BNM, Ossenkoppele R, Tolboom N, et al. Longitudinal Amyloid Imaging Using 11C-PiB: Methodologic Considerations. *J Nucl Med* 2013; 54: 1570–1576.
17. Logan J, Fowler JS, Volkow ND, et al. A strategy for removing the bias in the graphical analysis method. *J Cereb Blood Flow Metab* 2001; 21: 307–320.
18. Hardid J and Hilbe J. *Generalized estimating equations*. Chapman & Hall/CRC Press: Boca Raton, FL, 2012.
19. Gunn RN, Lammertsma AA, Hume SP, et al. Parametric imaging of ligand-receptor binding in PET using a simplified reference region model. *Neuroimage* 1997; 6: 279–287.
20. Catafau AM, Suarez M, Bullich S, et al. Within-subject comparison of striatal D2 receptor occupancy measurements using [123I]IBZM SPECT and [11C]Raclopride PET. *Neuroimage* 2009; 46: 447–458.
21. Jakoby BW, Bercier Y, Conti M, et al. Physical and clinical performance of the mCT time-of-flight PET/CT scanner. *Phys Med Biol* 2011; 56: 2375–2389.
22. Alves IL, Andrade MA, Reesink FE, et al. Theoretical insight into the relationship between SUV ratio and distribution volume ratio for a reference tissue model applied to [11C]-PIB brain PET. *Eur J Nucl Med Molecul Imag* 2014; 41: S187–S187.
23. Dutta J, Leahy RM and Li Q. Non-local means denoising of dynamic PET images. *PLoS ONE* 2013; 8: e81390. doi: 10.1371/journal.pone.0081390.
24. Kodaka F, Ito H, Kimura Y, et al. Test-retest reproducibility of dopamine D2/3 receptor binding in human brain measured by PET with [11C]MNPA and [11C]raclopride. *Eur J Nucl Med Mol Imaging* 2013; 40: 574–579.
25. Nyberg S, Farde L and Halldin C. Test-retest reliability of central [11C]raclopride binding at high D2 receptor occupancy. A PET study in haloperidol-treated patients. *Psychiatry Res* 1996; 67: 163–171.
26. Yoder KK, Albrecht DS, Kareken DA, et al. Test-retest variability of [11C]raclopride-binding potential in non-treatment-seeking alcoholics. *Synapse* 2011; 65: 553–561.
27. van Berckel BNM, Ossenkoppele R, Tolboom N, et al. Longitudinal amyloid imaging using 11C-PiB: methodologic considerations. *J Nucl Med* 2013; 54: 1570–1576.
28. Ferré J-C, Bannier E, Raoult H, et al. Arterial spin labeling (ASL) perfusion: Techniques and clinical use. *Diagn Interv Imag* 2013; 94: 1211–1223.
29. Koole JCM, Muylle T, Bormans G, et al. Optimized in vivo detection of dopamine release using 18F-Fallypride PET. *J Nucl Med* 2012; 53: 1565–1572.